Added note / *Nota añadida*: 20-11-2013
See erratum at the end of this file and at
ver fe de erratas al final de este documento y en
http://satori.geociencias.unam.mx/30-3/(11)Xu-ERRATUM.pdf

Structural analysis of a relay ramp in the Querétaro graben, central Mexico: Implications for relay ramp development

Shunshan Xu*, Ángel Francisco Nieto-Samaniego, Susana Alicia Alaniz-Álvarez, and Luis Mariano Cerca-Martínez

Universidad Nacional Autónoma de México, Centro de Geociencias,
Apartado Postal 1-742, Querétaro, Qro., 76001, México.
** sxu@geociencias.unam.mx*

ABSTRACT

This work presents a study of the overlapping zone between the Cinco de Febrero and Cimatario normal faults in the Querétaro graben, located in Querétaro, Mexico. The profiles measured from topographic fault scarps indicate that a relay ramp was formed in the southern part of the overlapping zone. In the relay ramp there are fractures striking oblique to the major faults. Those fractures are interpreted as Riedel fractures (R′) formed by minor rotation around a vertical axis. The orientation of bedding is not uniform in the relay ramp; dip directions of bedding are dependent on the sense and amount of rotation around two horizontal axes. The observed geometry of faults and bedding are consistent with published models of relay ramps in which there are three axes of rotation. Two axes are horizontal and one axis is vertical. For small faults, bedding rotations are due to both normal and reverse drags. In the relay ramp, bedding rotation due to simple shear is documented between the two large faults. On the other hand, the extension due to veins and dykes in the overlapping zone can reach 80 % of the total heave of the two overlapping faults. Finally, layer-parallel slip in the normal fault regime is occurring in the overlapping zone, despite the dips of bedding in our studied area being less than 20°.

Key words: relay ramp, normal fault, layer rotation, mechanism of rotation, Querétaro, Mexico.

RESUMEN

Se presenta el estudio estructural de la zona de traslape entre las fallas normales Cinco de Febrero y Cimatario que limitan el graben de Querétaro, ubicado en la ciudad de Querétaro, México. Los perfiles medidos en los escarpes topográficos indican que una rampa de relevo se formó en la parte sur de la zona de traslape. En la rampa de relevo se midieron fracturas cuyo rumbo es oblicuo a las fallas. Se interpretó que estas fracturas son Riedel (R′) formadas por efecto de una rotación cuyo eje fue vertical. La orientación de las capas no es uniforme a lo largo de la rampa de relevo y las direcciones de echado dependen del sentido y de la cantidad de rotación a lo largo de dos ejes horizontales. La geometría de las fallas y capas son consistentes con modelos publicados de rampas de relevo en las cuales actuaron tres ejes de rotación: dos ejes horizontales y uno vertical. Para fallas menores, las rotaciones de las capas son debidas a arrastre, tanto normal como inverso. Se documenta que en la rampa de relevo la rotación de las capas fue debida a cizalla simple entre las dos fallas principales. Por otro lado, se calculó que

la extensión causada por la intrusión de vetas y diques puede alcanzar el 80 % del total del rechazo horizontal causado por las dos fallas principales. Finalmente, se documentó en el área de estudio que hay deslizamiento paralelo a las capas, no obstante que la inclinación de ellas es ≤ 20°.

Palabras clave: rampa de relevo, falla normal, rotación de capas, mecanismo de rotación, Querétaro, México.

INTRODUCTION

When two normal faults have the same dip direction in their overlapping zone, a relay ramp may form to transfer displacement between them (Larsen, 1988). The reorientation or tilt of bedding in the relay ramp is the result of the decrease in displacement at the fault tips. The relay ramp may be breached with the development of a new structure (*e.g.*, Peacock and Sanderson, 1991; Huggins *et al.*, 1995; Kristensen *et al.*, 2008). The observed geometry of a relay ramp then represents only one stage in the evolution of the structure and the internal structure will vary according to the stage of fault growth.

Three different types of relay ramp have been distinguished: neutral, contractional, and extensional, depending on the nature of the strains within the relay ramp (Walsh *et al.*, 1999). The final orientation of bedding is dependent on the original attitude of beds in the relay zone and is also controlled by mechanical properties of stratified rocks and the types of drag near the faults (normal or reverse drag) (Peacock and Sanderson, 1994; Rykkelid and Fossen, 2002). In this way, the geometry of the relay ramp varies depending on the nature of bedding rotation (normal or reverse drag).

Fault linkage is a very important process during fault growth. Normal faults can grow by fault linkage across relay ramps at many scales. The relay ramps may be important locations for hydrocarbon (Larsen 1988), basin development (Anders and Schlische, 1994), and volcanic activity (Acocella *et al.*, 1999). This paper aims to study the bedding reorientation within the relay zone due to different mechanisms of layer rotation. The study area is the relay ramp between the Cinco de Febrero and the Cimatario normal faults in the Querétaro graben of the Trans-Mexican Volcanic Belt. This study focus on some parameters of a relay ramp in a quite simple geologic setting, so that many variables can be controlled.

GEOLOGIC BACKGROUND

The study area is located in the northern boundary of the central part of the Trans-Mexican Volcanic Belt (TMVB). The TMVB is an ~E–W active continental volcanic arc, 1200 km long across central Mexico. Volcanism in the TMVB is related to the subduction of the Cocos and Rivera plates beneath the North American plate (Ferrari *et al.*, 2000; Figure 1a).

Stratigraphic sequence

Previous authors described the stratigraphy of the Querétaro area, defining its evolution from Mesozoic to the present (*e.g.* Alaniz-Álvarez *et al.*, 2001, 2002; Carreón-Freyre *et al.*, 2005). The Cretaceous rocks consist of marine sedimentary rocks such as sandstone, limestone and siltstone (Alaniz-Álvarez *et al.*, 2001; Carreón-Freyre *et al.*, 2005). The Cretaceous limestone and siltstone unit crop out in the northern part of the study area (Figure 1b).

The Oligocene to Quaternary sequence in the Querétaro area is mostly characterized by a succession of basalt and andesite, which commonly occur interbedded with fluvio-lacustrine deposits. The range in age of this sequence is from *ca*. 12 to 5 Ma, based on isotopic dating of the volcanic rocks (Figure 1b, Aguirre-Díaz *et al.*, 2005). The lithostratigraphic column from bottom to top consists of (Figure 1):

(a) Andesite-basalt (ToA) crops out at the El Salitre village in northern Querétaro city (Figure 1b). The unit consists of andesitic lavas with intercalated breccias and pyroclastic deposits. The andesite is dark red and dark gray and its thickness varies from a few meters to 100 m (*e.g.*, Carreón-Freyre *et al.*, 2005). Rhyolitic dikes cut this sequence.

(b) Obrajuelo Dacite (Tdo) was first named by Alaniz-Álvarez *et al.* (2001). These rose-colored rocks are 100–200 m thick near Juriquilla and Santa Rosa de Jáuregui (Figure 1). The rocks have abundant andesine phenocrysts, along with K-feldspar and biotite.

(c) Ezequiel Montes Pyroclastic unit (TmTq) is a succession of unconsolidated pyroclastic rocks, rich in pumice, which was used in this work as a stratigraphic marker for measurement of the attitude of bedding. The Ezequiel Montes Pumice, described by Aguirre-Díaz and López-Martínez (2001) and Hernández *et al.* (2009), is formed of light gray pumice lapilli and ash, with interlayered surge deposits. The maximum thickness of this unit in the study area is 100 m and around Querétaro is only 5–10 m. The age proposed by Aguirre-Díaz and López-Martínez (2001) is 7.5–7.3 Ma based on the stratigraphic position of the deposit. The pumices were erupted from the Amazcala caldera, which is located 30 km to the NE of Querétaro city.

(d) Querétaro Basalt-Andesite (TAB) consists of lava flows that crop out on the top of most hills in the study area as small mesas. The rocks show black and dark grey colors. Its thickness is variable due to erosion. The youngest radiometric age of this sequence is 5.6 Ma (Figure 1b, Aguirre-Díaz *et al.*, 2005).

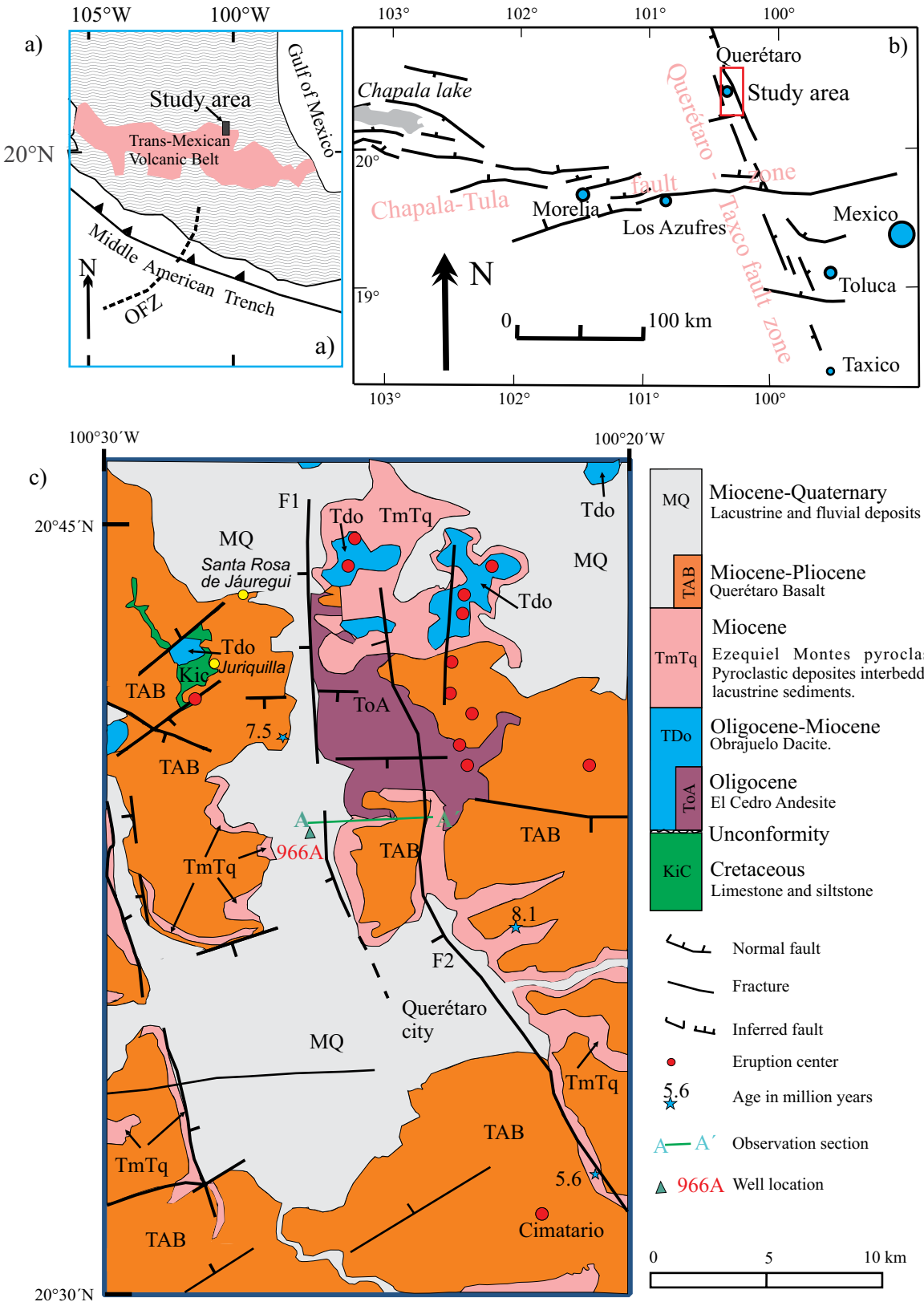

Figure 1. a) Map showing the tectonic location of study area. OFZ: Orozco fracture zone. b) The two fault zones located in the vicinity of the study area are shown c) Geologic map of the study area. F1: Cinco de Febrero fault; F2: Cimatario fault.

(e) The fluviolacustrine deposit (MQ) of Miocene-Quaternary age consists of conglomerate, and un-lithified gravel, sand, silt and mud that vary from poorly sorted to well sorted. Clasts are commonly angular to subangular. According to well records, the thickness of this unit varies from 20 to 150 m (Carreón-Freyre *et al.*, 2005).

Fault systems

The Querétaro graben is located at the intersection of two regional fault systems: (1) the NNW-oriented Taxco–San Miguel de Allende fault system (Alaniz-Álvarez *et al.* 2002), and (2) the Chapala–Tula fault system that strikes E–W to ENE and sub-parallels the length of the TMVB (Johnson and Harrison, 1990; Aguirre-Díaz *et al.*, 2005; Suter *et al.* 2001). The fault systems converge in the Querétaro region showing a near-orthogonal arrangement of normal faults in map view, yielding a mosaic of horsts, grabens, and half-grabens (Figures 1b, 2 and 3).

The Cinco de Febrero and Cimatario faults trend NNW with lengths of 37 km and 66 km, respectively (Figure 3). The Querétaro graben is bounded to the east by the Cimatario fault. For these two faults, the footwall blocks lie to the east. The dips of the faults vary from 60° to 80° west.

From the Miocene to the Recent, three main periods of fault activity are recognized in the region, which occurred at 10 Ma, 7 Ma, and in the Quaternary (Alaniz-Álvarez *et al.* 2001, 2002). The intermittent activity of these two fault systems was documented by Dávalos-Álvarez *et al.* (2005) in the Huimilpan region, and has been explained by permutations between the intermediate and least principal stresses (Suter *et al.*, 1995). Aguirre-Díaz *et al.* (2005) considered that NNW faults are related to the Basin and Range stress regime, and ENE faults to the Mexican Volcanic Belt intra-arc stress regime. For these authors, the two stress provinces overlap at the Querétaro area and, consequently, the NNW faults and ENE faults cross-cut each other. In contrast, using the theory of fault reactivation, Alaniz-Álvarez *et al.* (2001, 2002) proposed that both, the NNW faults of the Taxco–San Miguel de Allende fault system and the E–W faults of the Chapala–Tula fault system, can be active simultaneously in the Quaternary under the stress field active in the TMVB, producing oblique extension to both systems at the same time. These authors argued that the Basin and Range stress regime was active until Miocene times in this region, whereas the TMVB intra-arc stress regime has been active in the Pliocene-Quaternary. A complete discussion of this topic can be found in Alaniz-Álvarez *et al.* (2002).

Alaniz-Álvarez *et al.* (2001) reported a vertical displacement of 100 m for the Cinco de Febrero fault, and a mean displacement of 80 m for Cimatario fault. In the present study, we observed that the Cinco de Febrero fault is characterized by steps, having 172 m of total vertical displacement (Figure 2). Fault breccias are commonly observed in the fault damage zones (Figure 2).

DISPLACEMENT PROFILES OF THE CINCO DE FEBRERO AND CIMATARIO FAULTS ESTIMATED FROM TOPOGRAPHIC SCARPS

Measurement method

We used topographic fault scarps to estimate the vertical displacements of Cinco de Febrero and Cimatario faults. For this purpose, we used a digital elevation model obtained from the Instituto Nacional de Estadística, Geografía e Informática (INEGI) website (Figure 3a). Two large faults show topographic relief within the resolution of the images. The software Global Mapper v9.02 (http://www.globalmapper.com) was used to measure the topographic differences across the strikes of the faults. In order to avoid major errors in measurement, care was taken to select sections across the faults that are not cut by streams nor lie in the vicinity of volcanic vents. In spite of these precautions, the obtained values may be underestimated due to erosion of the foot

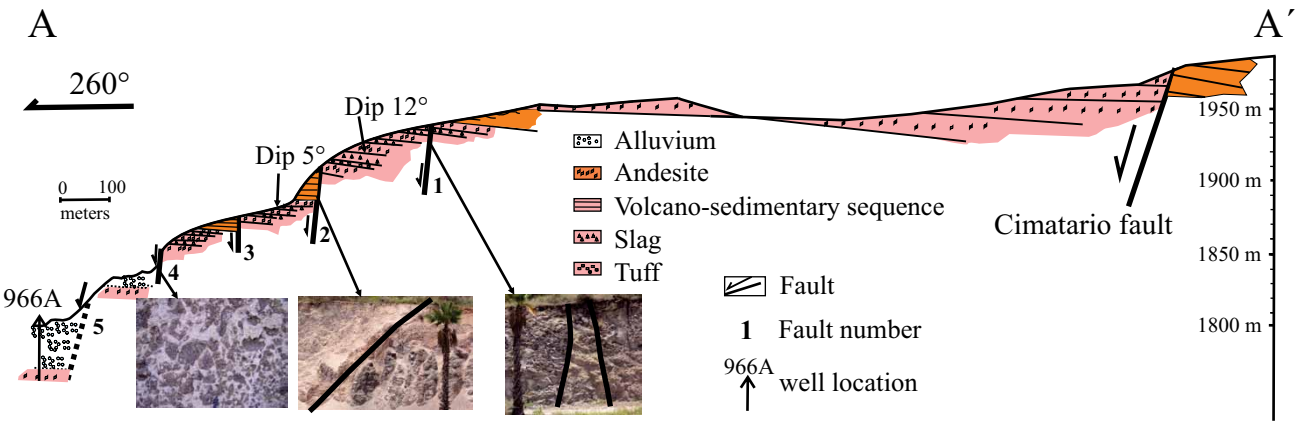

Figure 2. Geological cross-section A-A' whose position is shown in Figure 1c. The Cinco de Febrero fault is characterized by steps formed by four faults with high-angle dips.

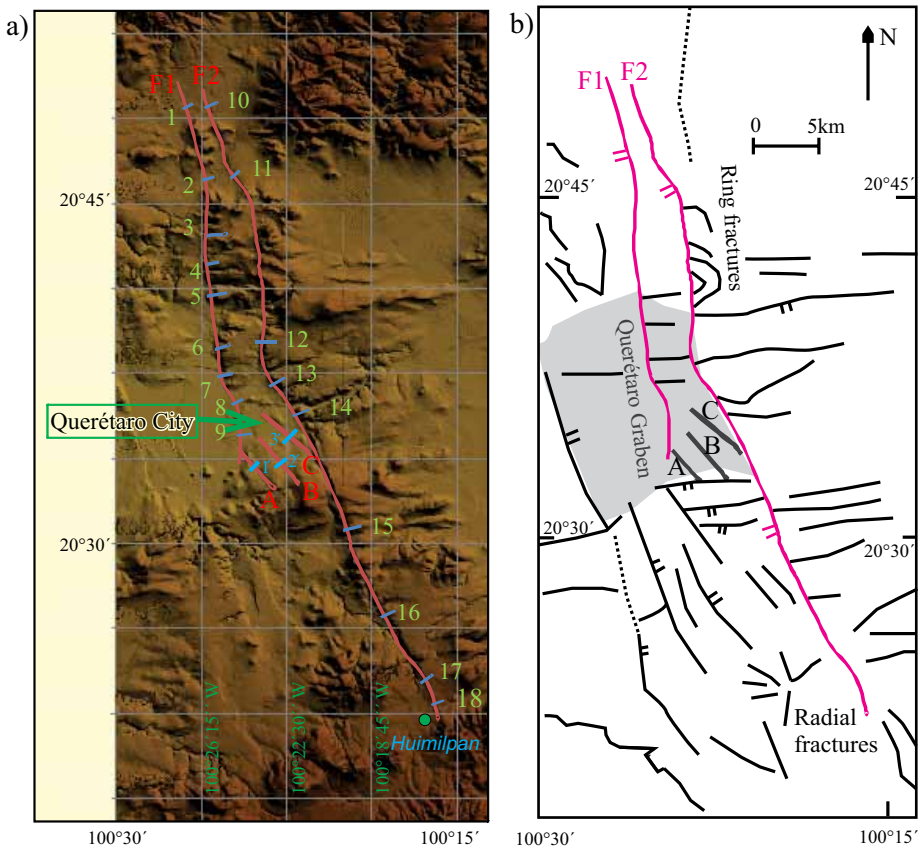

Figure 3. a) Digital elevation model of the Querétaro city and vicinity. The morphology of the NNW and ENE fault scarps north and south of Querétaro city can be clearly distinguished. F1: Cinco de Febrero fault; F2: Cimatario fault. The blue short lines indicate the position of the topographic sections. Digits in green color represent section numbers. A, B, and C are Riedel type fractures (R´) formed as result of rotation of the vertical axis in the relay zone. b) Fractures interpreted from the digital elevation model in (a); the Querétaro graben is marked by gray shaded area.

walls and to sedimentation in the hanging walls. In general, the thickness of erosion on the footwall and sedimentary thickness on the hanging wall are not equal. To estimate the error of true vertical displacement from topographic relief, we compare the topographic section 5 in Figure 4 and section A-A´ observed in the field (Figure 2). In section A-A´, the vertical displacement obtained from surface observation is 96 m. If only the thickness of the Quaternary fluviolacustrine deposit (at least 20 m according to Carreón-Freyre *et al.*, 2005) and the stratigraphic marker Ezequiel Montes Pumice within the Querétaro graben are considered, a conservative estimation of the vertical displacement of about 150 m is obtained. By comparing with the geological record of well number 966A drilled by Petroleos Mexicanos (PEMEX), the obtained vertical displacement is 172 m. The well location is about 500 m from section A-A´ (Figure 1); the vertical displacement of 172 m is estimated by projecting the top bedding ToA on the cross-section A-A´ from well 966A. On the other hand, the topographic difference from section 5 in Figure 4 is 137 m. In this way, we can conclude that the topographic difference is 80 % of the real vertical displacement near the field-based control section.

In this work, the topographic difference across the faults is called the topographic displacement. As described above, the topographic displacement estimated in the control section is less that the real vertical displacement. In spite of this, we assumed that the form of the topographic displacement profile along the fault resembles the true vertical displacement profile. Based on this assumption, to obtain topographic displacement profiles, we measured the displacements in 18 cross-sections, nine across the Cinco de Febrero fault and nine across the Cimatario fault (Figure 4). The maximum topographic displacement is 153 m for the Cinco de Febrero fault, and 158 m for the Cimatario fault.

Features of the topographic displacement profiles

Displacement is zero at the fault tips and commonly reaches a maximum near the center (*e.g.*, Dawers *et al.*, 1993). For any two overlapping normal fault segments, the fault-displacement distribution in the overlap zone depends on the initial configuration of the faults (Maerten *et al.*, 1999). Displacement geometries and displacement gradients of a single isolated fault can be used as reference for studying an overlapping zone.

The Cinco de Febrero and the Cimatario faults form an overlapping zone in the northern part of Querétaro city.

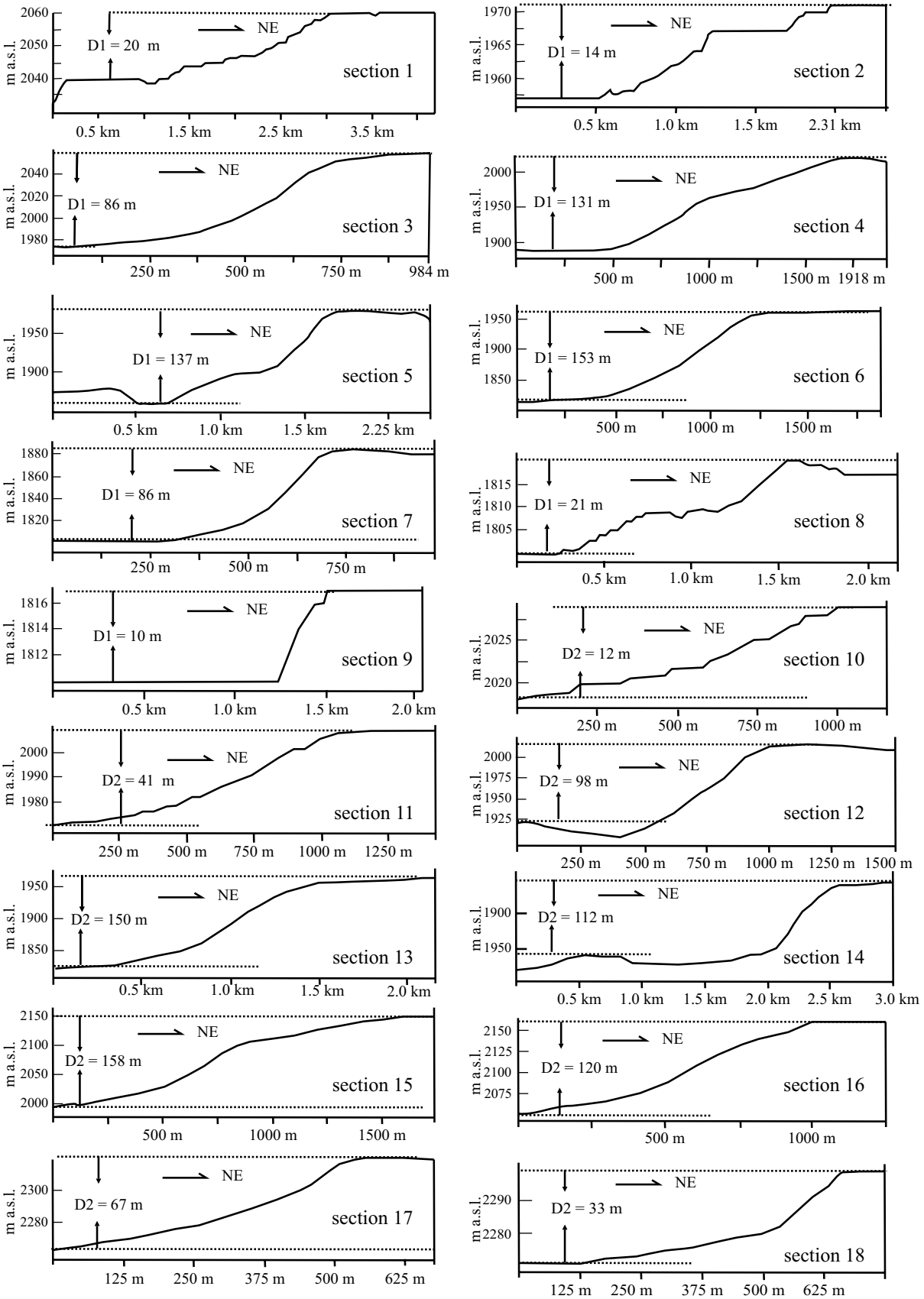

Figure 4. Topographic sections across the Cinco de Febrero and the Cimatario faults measured with Global Mapper v9.02. The section positions are shown in Figure 3a. D1 and D2 correspond to the topographic displacement of the Cinco de Febrero and Cimatario faults, respectively; masl indicates the meters above sea level.

The spacing between the two faults is 5–8 km and their total length is about 67 km. The spacing/total length ratio is 8 % – 12 %. The degree of fault interaction between pairs of faults can be quantified by the ratio of spacing to total length (*e.g.*, Gupta and Scholz, 2000; Hus *et al.*, 2005). Gupta and Scholz (2000) proposed that two normal faults interact when the ratio of spacing to their total length is less than 15%. Based on the spacing/total length ratio in the studied area and the critical value, we conclude that interaction between the two faults in the area is possible. The topographic displacement profiles for the two faults are shown in Figure 5. In the overlapping zone, two parts are distinguished in the profiles. In the northern part of the overlapping zone, the displacement gradients for both faults decrease northward. This characteristic of the displacement distributions on two faults is similar to that found in two parallel normal faults with no relay ramp. In this way, there is no transfer displacement between faults in this part. Therefore, we consider that this part do not form a typical relay ramp. In the southern part of the overlapping zone, the displacement gradient for the Cimatario fault increases to the south, while the displacement for the Cinco de Febrero fault decreases to the south. This feature is similar to the displacement profile in a typical relay zone (*e.g.*, Peacock

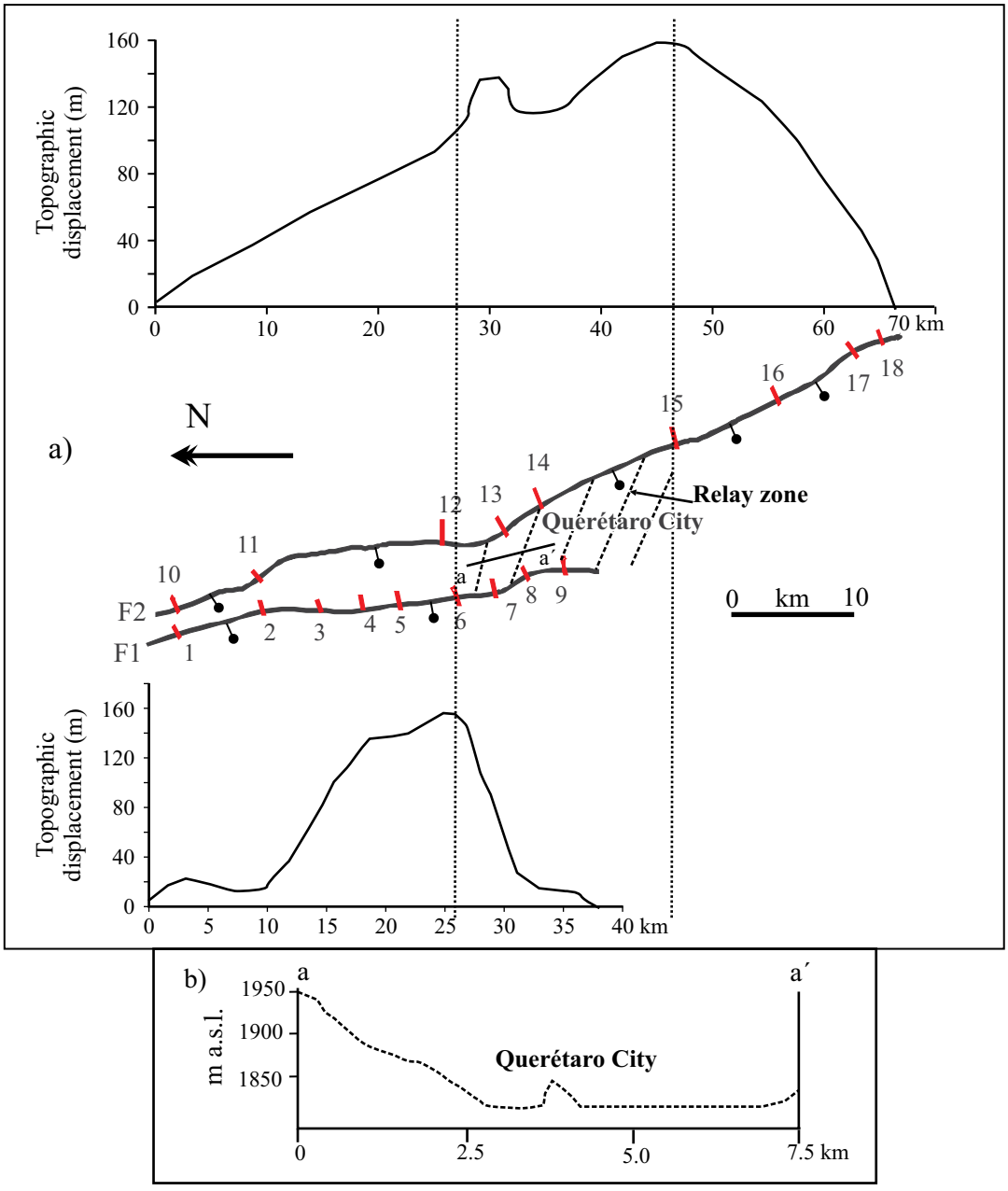

Figure 5. a) Topographic vertical displacement profiles of the Cinco de Febrero and the Cimatario faults. In the overlapping zone, the southern part shows the typical features of a relay ramp. b) Topographic section, whose location is shown in (a).

and Sanderson, 1991; Soliva and Benedicto, 2005). On the basis of the above observations, the following sections will mainly emphasize on the structural analysis of the southern part of the overlapping zone.

A large relay zone can be distinguished from the ramp observed in the digital elevation model (*e.g.*, Crider and Pollard, 1998). Our results show that Querétaro city is located in the relay ramp between the Cimatario and Cinco de Febrero faults. This can be seen in the topographic profile a – a', which crosses the main part of Querétaro city (Figure 5). The slope of the relay ramp is 2°. This value is smaller than the dips of bedding in the Ezequiel Montes Pumice (TmTq) (5° to 12°). There are two reasons why the slope of the ramp is less than the bedding that controls the ramp. One reason is the erosion of the higher part of the ramp and sedimentation in the low part. The other reason is that the direction of the profile is not parallel to the dip direction of bedding. The apparent dip β' on the bedding parallel to the relay zone can be calculated by:

$$\beta' = \text{Arc tan } [(\tan \beta)(\cos \gamma)] \quad (1)$$

where γ is the intersection angle between the strike of the fault and the dip direction of the bed, and β is the measured dip. The calculated apparent dip varies from 3° to 10°.

DEFORMATION OF BEDS IN THE RELAY RAMP

Bedding rotation in the relay ramp

In a relay ramp, three axes of rotation occur for the horizontal beds (Figure 6; Ferrill and Morris, 2001). As shown in Figure 6, the horizontal axis (1) is parallel to the strike of the faults. The rotation around horizontal axis 1 may be responsible for the vertical component of displacements. The horizontal axis 2 is perpendicular to the fault strike. The rotation around horizontal axis 2 accommodates the transfer of displacement between segments. The horizontal components of displacement along the two faults in the relay zone produce horizontal rotation of the relay zone. We define this rotation axis as vertical axis 3. The rotation of the vertical axis does not produce changes in dips of bedding, but it can produce fractures in the relay ramp. In the study area, the Riedel type fractures (R´) are interpreted to have formed in response to minor rotation around vertical axis in the relay zone. The fractures R´ commonly have an angle 70° with the principal shear direction (Figure 6a). These fractures in the relay zone trend NNW and are labeled in Figure 3a (fractures A, B, C). The topographic sections across these Riedel fractures are nearly symmetric (Figure 7). This characteristic implies that the fractures have no or only a little vertical displacement. They may be lateral faults or "shear fractures" (fracture R´). As the relay ramp grows, these fractures will have normal displacements and become normal faults. When these minor normal faults connect the two first-order faults, the relay ramp will be breached (Peacock and Parfitt, 2002). This process is common for relay ramps to become cut by the minor faults of this orientation.

For horizontal axis 1, there are two opposite directions of rotation or tilt of bedding, depending on the mechanism of drag structure. The sense of rotation is dependent on the observation direction. These scenarios are shown in Figures 8a, 8b and 8c. In the case of Figure 8a, normal drag produces the rotation of bedding around axis 1. The direction of rotation is then counterclockwise. Normal drag is usually considered to be formed prior to faulting as the fault propagates up into the fold formed above the fault (*e.g.*, Groshong, 1999; Rykkelid and Fossen, 2002). Rykkelid and Fossen (2002) summarized other cases of normal drag. They may be folds in the hangingwall of anti-listric fault,

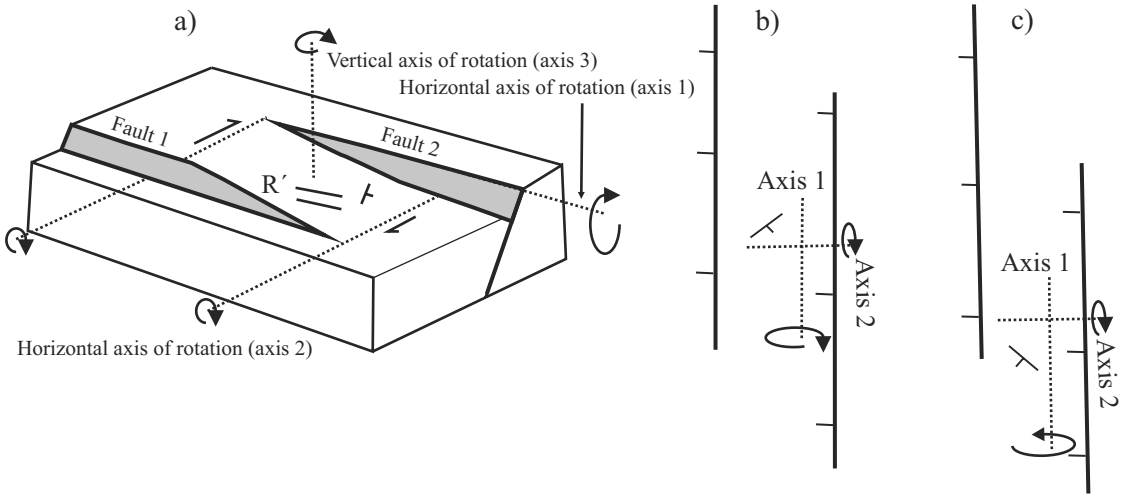

Figure 6. a) Three dimensional sketch showing the structure in a relay zone. Three axes of rotation are shown (modified from Ferrill and Morris, 2001). R´: Riedel fractures due to rotation of the vertical axis. b) and c) are two dimensional sketches showing two combinations of rotation around axis 1 and axis 2, which cause different orientations of bedding in the relay zone.

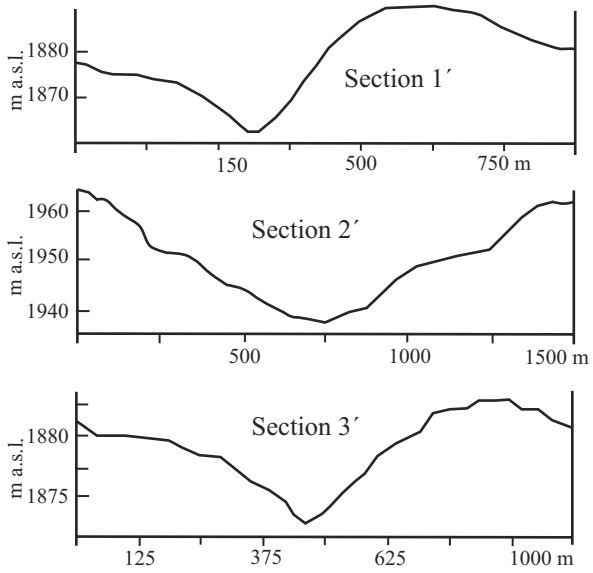

Figure 7. Topographic sections across the Riedel fractures R´ (A, B, C; Figure 3a) measured with Global Mapper v9.02.

frictional drags, lithology controlled drags, etc. In the case of Figure 8b, the bedding rotation around axis 1 is due to rigid body rotation. In this way, the rotation occurs across the zone and it is clockwise. In Figure 8c, the bedding rotation around axis 1 is due to vertical shear or inclined shear (Westaway and Kusznir, 1993; White *et al.*, 1986; Xu *et al.*, 2004). For the simple shear mechanism, the vertical shear or inclined shear is distributed. This implies that deformation near the fault plane is larger than that far from the fault plane (Westaway and Kusznir, 1993; White *et al.*, 1986; Xu *et al.*, 2004). The bedding rotation for the same bed can be both clockwise and anticlockwise for the same observation direction as shown in Figure 8c.

For different fault-drag mechanisms, there are different combinations between axis 1 and axis 2 (Figure 6b and 6c). The dip direction of bedding is to the upper-left if the rotation around axis 1 is clockwise and the rotation around axis 2 is anticlockwise (Figure 6b). On the other hand, the dip direction of bedding is to the lower-left if the rotation around both axis 1 and axis 2 are anticlockwise (Figure 6c). In this way, the attitude of bedding in the relay zone varies depending on the senses of the rotation around two horizontal axes.. We measured the attitudes of bedding from one cross-section in the relay ramp of the northern Querétaro city (Figure 9). The dip directions at points P1 and P5 are similar to the model of Figure 6b, whereas those at points P2, P3 and P4 are consistent with the model of Figure 6c Therefore, the distribution of dip direction in this section indicates a simple shear mechanism (vertical or inclined shear) for layer rotation during faulting. This mechanism has been documented in other volcanic areas in Central México (Xu *et al.*, 2004). On the other hand, in the study area, both normal and reverse drags are observed for small faults (Figures 8d and 8e). These results indicate that for the same layers there is not a unique mechanism of drag for beddings. The mechanism of drag of bedding is controlled by mechanic properties and faulting process. Weak rocks has a tendency to produce simple shear. On the other hand, the mechanic properties of the strata are dependent on the length or width that is involved. The strata that produce simple shear across a wide zone (large fault space) may produce rigid body rotation across a narrow zone (minor fault space). This is similar to the beam deformation, for which a longer beam is more easily folded but not faulted

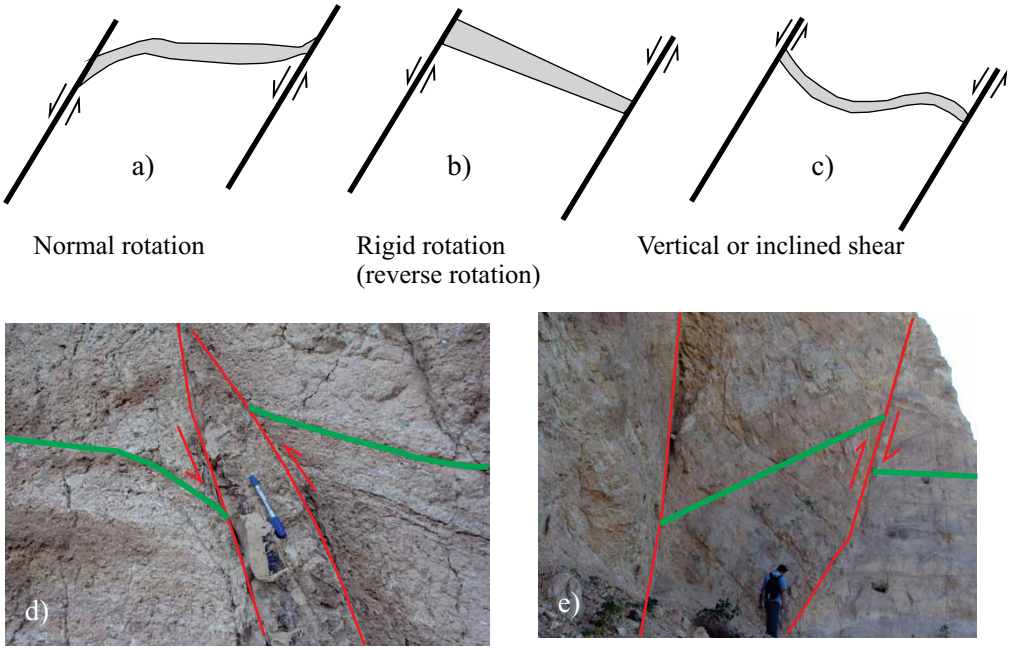

Figure 8. Three mechanisms of layer rotation for normal faults are shown in a)-c). Normal and reverse drags are observed in d) and e), respectively.

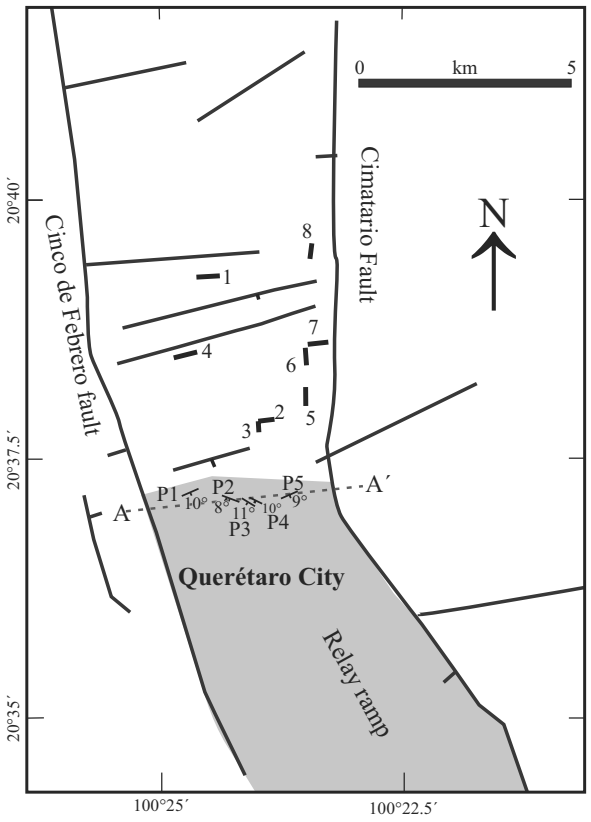

Figure 9. Attitude of layers across the section A-A´ in the southern relay zone located in the northern Querétaro city. The distribution of bedding orientations indicates that simple shear occurred during normal faulting. Thick black lines with digit indicate the position of sections considered for calculating the extension due to small veins and dykes. P1 to P5 are the locations where the attitude of bedding was measured.

than a shorter beam. Also, the mechanic properties of the strata change with temperature and confining pressure. In Figure 8d, the fault was companied by the intrusion of a dike, which would have resulted in higher temperature than general conditions without dikes. In this case, the bedding may produce simple shear near the dike-fault as shown in Figure 8d.

Calculation of extension due to veins and dykes

Extensional strain is usually accommodated by discrete structures such as joints, veins and faults (Wojtal, 1989; Segall and Pollard, 1983). Fault strain can be estimated from fault slip or directly from displacement of faults (Peacock and Sanderson, 1993). Vein strain can only be estimated from thickness of veins.

In the study area, we observed calcite and gypsum veins. Four types of calcite vein structures were identified in the study area. The first type of calcite veins has oriented bands parallel to vein walls (Figure 10a). They might have form from post-magmatic hydrothermal solutions at high temperature. The second type of calcite veins correspond to brecciated veins (Figure 10b). The fragments in these veins are from the host volcanic rocks or calcite itself. The third type of calcite veins expresses no internal structure but shows different generations of calcite growth, with different colors (Figure 10c). The fourth type of calcite veins has a botryoidal crust and a bright white color (10d).

On the other hand, there are two types of dykes according to composition and structures. One correspond to volcanic dykes, which generally are dark green or grey andesite and dark red rhyolite (Figure 10e). The second one are pyroclastic dykes (Figure 9f) with variable colors, and thickness from a few centimeters to tens of centimeters. The veins and dykes usually form swarms (Figures 10g and 10h). Their strikes are usually sub-parallel to the two main sets of faults. This feature allows us to conveniently calculate extension due to the filling of veins and dykes.

Because the veins and dykes are not exactly perpendicular to the section and are not vertical, the thickness of the veins and dykes cannot be directly used to calculate the extension. The corrected thickness (W), named as width of veins or dykes in this study, is calculated as follows:

$$W = T \sin \alpha \quad (2)$$

where T is the thickness of the vein in the observation section and α is the apparent dip angle of vein or dyke. The extension is calculated with the equation:

$$e = (\sum W)/(L-\sum W) \quad (3)$$

where L is the length of section.

Due to city constructions and scarcity of outcrops, we cannot measure a complete section across the Cinco de Febrero and Cimatario faults. In spite of this, eight shorter sections were measured, four of which are nearly north-south, and the other four sections are nearly west-east (Figure 9). The calculated results are shown in Table 1. Extension is quite small, varying from 0.005 to 0.037. For the north-south sections, the extension near the relay ramp (Section 3) is relatively larger. Similarly, for the west-east sections, the extension near the relay ramp (Section 2) is relatively larger as well. These results indicate that the relay ramp is a zone with more intensive deformation.

If we assume that he calculated extensions in the short west-east sections represent the extension of the whole width between faults (S) across the relay zone (between the Cinco de Febrero and Cimatario faults), the horizontal width filled by veins and dikes (Ls) can be calculated by $Ls = S\,(e/(e+1))$. For example, the extension for section 2 is 0.023, the measured spacing (width) S in this position is 5000 m, then the calculated horizontal extensional value (Ls) is 112 m. On the other hand, the heaves of the two faults near this section can be approximated to $h = V/\tan\theta$, where V is the vertical topographic difference, and θ is the dip angle of the fault. The total value of V is 260 m near section 2 for two faults. Based on these

Figure 10. a) Calcite vein with bandings. b) Calcite vein with rhyolitic fragments (red color). c) Calcite vein with two generations of crystals (black and dark green). d) Calcite vein with botryoidal crust. e) Pyroclastic dyke. (f) andesitic and rhyolitic dyke. g) Parallel calcite veins. h) Parallel pyroclastic dyke.

values, the total heaves for the two faults is h = 150 m, assuming that the dips of faults are 60°. In this way, Ls/h = 0.7488 = 74.88 %. This result implies that the total extensional value in the relay zone due to small veins and dykes is *ca*. 75 % of total heave of the two overlapping faults. As described above, the topographic difference is always less than the real vertical displacement. This implies that the real ratio of Ls/h is less than, but probably close to, 80 %.

Layer-parallel slip

The layer-parallel planes of bedding are commonly weak planes. These planes would be reactivated if the stress on them reaches the critical condition of reactivation (*e.g.*, Alaniz-Álvarez *et al.*, 1998). According to the Mohr-Coulomb theory, for a pre-existing plane, the critical condition to slip is:

$$\tau = C + \mu\sigma \quad (4)$$

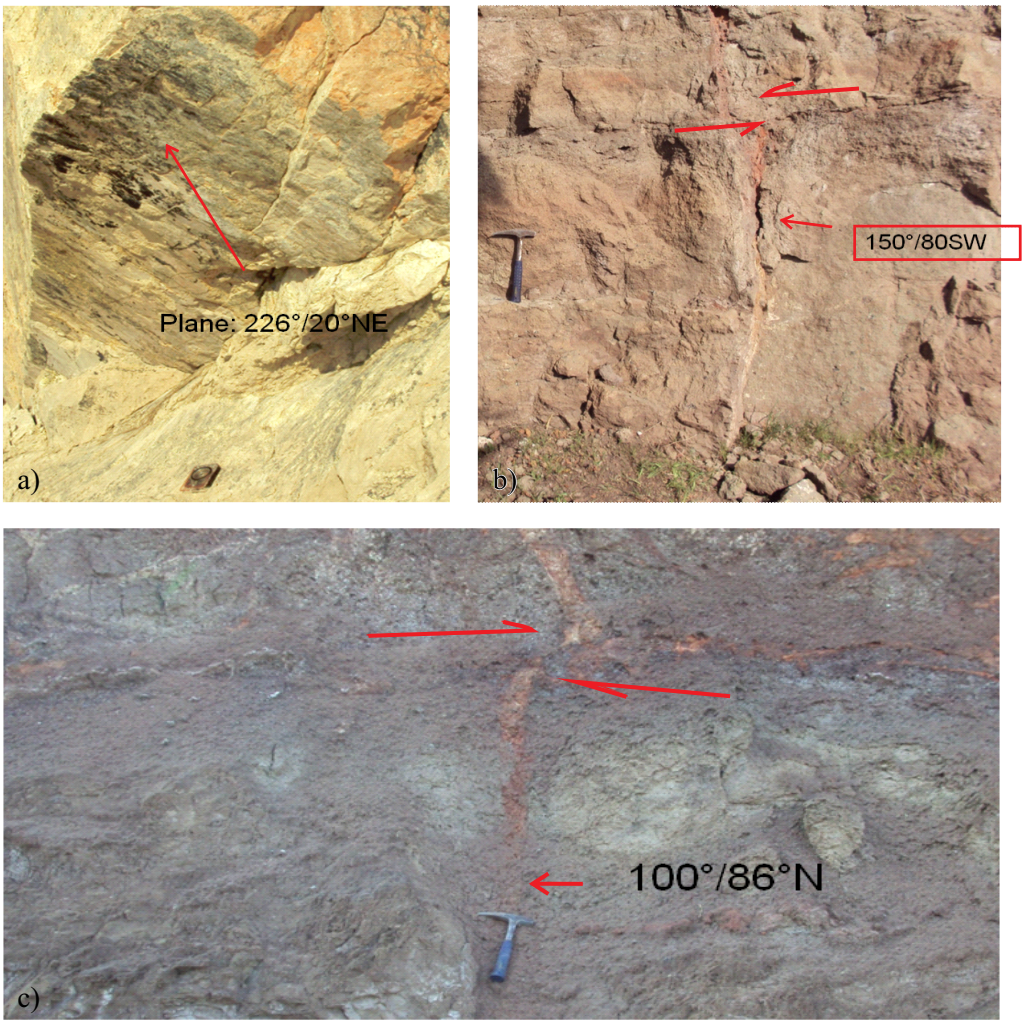

Figure 11. Layer-parallel movement observed in the field. a: Slickenlines on the layer-parallel plane. b and c: layer-parallel slip that cuts pyroclastic dykes.

where τ is shear stress and σ is normal stress on the pre-existing plane; C is the shear strength on the pre-existingplane when σ is zero, and μ the coefficient of friction on the pre-existing plane.

Layer-parallel slip is observed in our study area (Figure 11). In Figure 11a, slickenlines on the layer-parallel plane are observed. In Figures 11b and 11c, the layer-parallel planes dislocate small volcanic dykes. As seen in Figure 11, the dips of the layer-parallel planes are typically less than 20°. Generally, the low-angle planes are difficult to reactivate under a normal fault regime. However, reactivated low-angle planes have been reported in published work (*e.g.*, Allmendinger *et al.*, 1987). Alaniz-Álvarez *et al.* (1998) documented that planes with dips of 10° can be reactivated in a normal fault regime under favorable conditions. Higgs *et al.* (1991) observed that layer-parallel simple shear is associated with extensional faulting. The reactivated low-angle planes can be also seen in the Mohr diagram. In a Mohr diagram, the minimum angles of the reactivated planes are dependent on the magnitude of the values of C and μ (Xu *et al.*, 2010). If the values of C and/or μ are small enough, then planes less than 20° can be reactivated in a normal fault regime.

DISCUSSION

Effect of E-W to ENE fault system on the topographic displacement

As mentioned above, there are two fault systems in the study area, of which, the faults oriented E–W to ENE belong to the Chapala-Tula fault system. The activity of this fault system may produce drags of bedding in the relay zone. In this way, near the ENE to E-W faults, the bedding orientation results from the combined effects of the NNW to N-S and ENE to E-W faults. One possible combination is shown in Figure 12. In the absence of an E-W fault, the bedding near the N-S fault may dip to the east (Figure 12a). Where an E-W fault is present, the bedding dips to

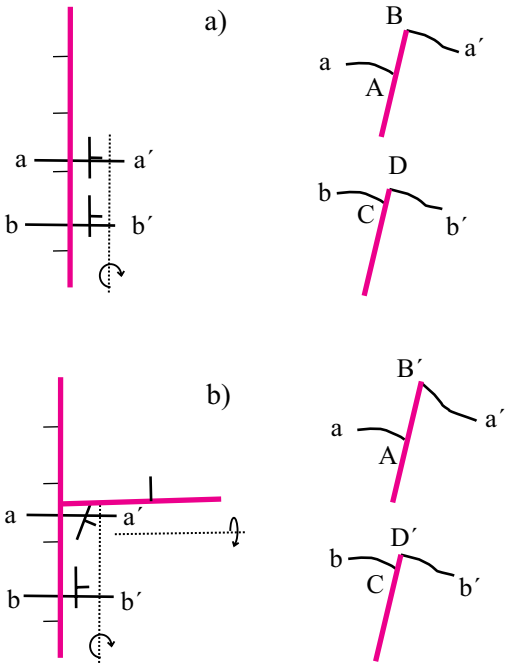

Figure 12. Effect of E-W faults on topographic displacements. For the cross-section near the E-W fault (a-a´ in figure b), the displacement changes because of fault drag. It is seen that AB´ in b) is larger than AB in a).

the southeast because of the superimposition of bedding tilt produced by the E-W fault (Figure 12 b). As a result, in the locations where bed rotations due to the activity of two faults are combined, the displacement across the N-S fault decreases or increases. For example, when comparing the Figures 12a and 12b, we can see that the displacement AB´ in Figure 12b is larger than the displacement AB in Figure 12a along cross-section A-A´. To avoid the effect of the E-W to ENE fault system on topographic displacements, the topographic cross-sections across the two main faults were selected as far from the E-W faults as possible (Figure 3a). On the other hand, because the length of E-W to ENE faults is shorter than that of NNW faults, the bedding tilt produced by the E-W to ENE faults is smaller than that by the NNW faults. Therefore, the effect of E-W to ENE fault system on the topographic displacement across N-S faults is not very strong in the studied ramp.

Slickenline directions on NNW faults

Active pure-dip or oblique normal faults can make a large difference in how secondary structures form (Crider 2001). Then, fault-slip data are important for analyzing the linkage of a relay ramp. According to Aguirre-Díaz *et al.* (2005), the directions of the fault-slip on both the NNW and ENE sets are nearly 90°. On the basis of paleostress inversion using fault-slip data, they obtained a principal extension oriented ENE for NNW faults and a NNW principal extension for the ENE faults. From our fieldwork, we also observed that the slickenlines on NNW faults also show nearly dip slip (Figure 13).

Growth stage of the relay ramp in the area

A relay ramp develops by stages during fault growth. Any observed relay ramp then represents one stage in its

Figure 13. Photographs of slickenlines on NNW faults. a: Side view to the SSE of a minor NNW fault parallel to the main fault plane; the fault was observed along cross-section A-A´ shown in Figures 1b and 2. The layered sequence is the Ezequiel Montes Pumice and interbedded deposits of reworked pumice. (b) Front view to the east of a NNW fault in the north part of the Querétaro city.

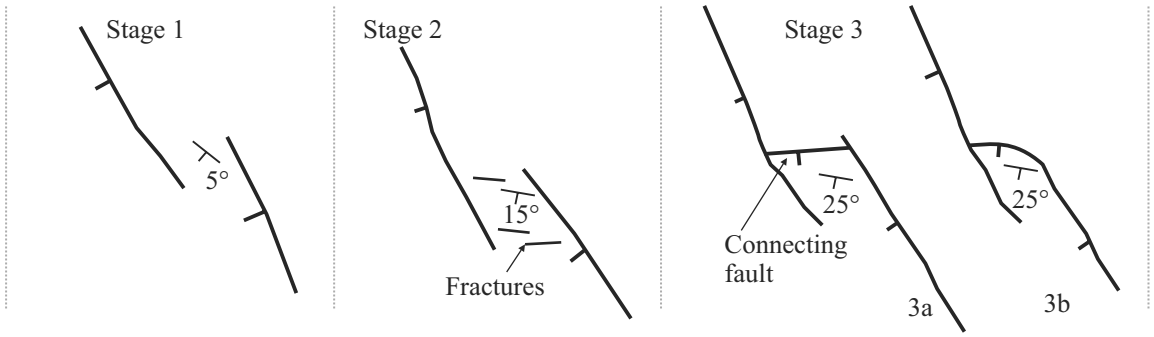

Figure 14. Sketch showing the development stages of a relay ramp. At stage 1, the two faults understep and little rotation of the bedding occur in the relay zone. At stage 2, two faults overlap and the relay ramp has higher bedding dips than at stage 1. At stage 3, two faults are linked and become one larger fault. Two ways of linkage can be distinguished: plane to plane (3a) and tip to plane (3b).

evolution. The growth of a relay ramp is common divided into three stages (Acocella *et al.*, 2000; Peacock and Parfitt, 2002): understep stage, overstep stage, linkage stage (Figure 14). There are two ways of fault linkage: plane-to-plane linkage and tip-to-plane. For plane-to-plane linkage, two overlapping fault segments are linked by one or more connecting faults. For tip-to-plane linkage, one segment is curved towards the other segment to connect with it at a branch point. At stage 1, two faults have no overlapping zone and, in the relay zone, the beddings have low dips. The two normal faults may be connected above or below the mapped level (Peacock and Parfitt, 2002). At stage 2, two faults have an overlapping zone, for which the relay ramp shows moderate bedding dips (10°–20°). Also, the relay ramp has more intensive fractures than in the nearby area. At stage 3, some fractures gradually obtain normal displacement and become thoroughgoing faults. The relay ramp is breached as the bedding dips and displacement increase.

In our study area, the dips of bedding vary from 5° to 20°. Average bedding dip is 10°, which is a moderate value in a relay ramp (Peacock and Parfitt, 2002). On the other hand, the fractures in the ramp have little normal displacement. These structures indicate that the relay ramp is at stage 2 of its evolution.

CONCLUSIONS

The Cinco de Febrero and Cimatario faults in the Querétaro graben show NNW strikes and are 37 km and 66 km long, respectively. In the northern part of the overlapping zone, the displacement gradients on two faults decrease to the same direction (northward), which implies this part is not a typical relay ramp. In the southern part of the overlapping zone, the displacement gradient on one fault increase to the south while the displacement on the other fault decreases to the south. We consider that this part is consistent with a typical relay ramp. In the relay ramp, Riedel fractures (R´) are interpreted to have formed by rotation around a vertical axis. The dip directions of bedding in the relay ramp are dependent on the sense and amount of rotation around two horizontal rotation axes. For small faults, the bedding rotations are due to both normal and reverse drags. For the two large faults, the bedding data from the section in the relay ramp indicates that a simple shear mechanism (vertical or inclined shear) occurred for layer rotation during faulting. These results indicate, for the same layer, that the drag mechanism can be different for different faults. On the other hand, the extension estimated from small veins and dykes indicate that extension in the relay ramp is larger than in other locations of the overlapping zone, which implies a more intensive deformation in the relay ramp. In the studied section, extension due to veins and dykes can reach 80% of total heave produced by the two overlapping faults. The other type of deformation in the overlapping zone is layer-parallel slip. This type of slip in the normal fault regime requires that the values of C and/or μ for the layers are quite small.

ACKNOWLEDGEMENT

This work was supported by 89867 and 80142 Conacyt grants and IN107610 PAPIIT grant of UNAM. Marcos González Hernández helped with the fieldwork. Also, we appreciate the pertinent comments on the paper by Gabriel Chávez Cabello, Thierry Calmus and an anonymous reviewer.

REFERENCES

Acocella, V., Salvini, F., Funiciello, R., Facenna, C., 1999, The role of transfer structures on volcanic activity at Campi Flegrei (southern Italy): Journal of Volcanogy and Geothermal Research, 91, 123-139.

Acocella, V., Gudmundsson, A., Funiciello, R., 2000, Interaction and linkage of extension fractures and normal faults: examples from the rift zone of Iceland: Journal of Structural Geology, 22, 1233-1246.

Aguirre-Díaz, G.J., López-Martínez, M., 2001, The Amazcala caldera, Querétaro, México. Geology and geochronology: Journal of

Volcanology and Geothermal Research, 111, 203-218.

Aguirre-Díaz, G.J, Nieto-Obregón, J., Zúñiga, R., 2005, Seismogenic Basin and Range and intra-arc normal faulting in the central Mexican Volcanic Belt, Querétaro, México: Geological Journal, 40, 1-29.

Alaniz-Álvarez, S.A., Nieto-Samananiego, A.F., Tolson, G., 1998, A graphical technique to predict slip along a preexisting plane of weakness: Engineering Geology, 49, 53-60.

Alaniz-Álvarez, S.A., Nieto-Samaniego, A.F., Reyes-Zaragoza, M.A., Ojeda-García, A.C., Orozco-Esquivel, M.T., Vasallo, L.F., 2001, Estratigrafía y deformación extensional en la región San Miguel de Allende-Querétaro, México: Revista Mexicana de Ciencias Geológicas, 18, 129-148.

Alaniz-Álvarez, S.A., Nieto-Samaniego, A., Reyez-Zaragoza, M.A., Orozco-Esquivel, T., Ojeda-García, A.C., Vassallo, L.F., Xu, S-S., 2002, El sistema de fallas Taxco-San Miguel de Allende: implicaciones en la deformación post-eocénica del centro de México: Boletín de la Sociedad Geológica Mexicana, 55, 12-29.

Allmendinger, R.W., Hauge, T.A., Hauser, E.C., Potter, C.J., Klemperer, S.L., Nelson, K.D., Knuepfer, P., Oliver, J., 1987, Overview of the COCORP 40°N transect, western United States: the fabric of an orogenic belt: Geological Society of America Bulletin, 98, 308-319.

Anders, M.H., Schlische, R.W., 1994, Overlapping faults, intra-basin highs and the growth of normal faults. Journal of Geology, 102, 165-180.

Carreón-Freyre, D., Cerca, M., Luna-González, L., Gámez-González, F.J., 2005, Influencia de la estratigrafía y estructura geológica en el flujo de agua subterránea del Valle de Querétaro: Revista Mexicana de Ciencias Geológicas, 22(1), 1-18.

Crider, J.G., 2001, Oblique extension and the geometry of normal fault linkage: mechanics and a case study from the Basin & Range in Oregon: Journal of Structural Geology, 23, 1997-2009.

Crider, J.G., Pollard, D.D., 1998, Fault linkage: three-dimensional mechanical interaction between echelon normal faults: Journal of Geophysical Research, 103, 24373-24391.

Dávalos-Álvarez, O.G., Nieto-Samaniego, A.F., Alaniz-Álvarez, S.A., Gómez-González, J.M., 2005, Las fases de deformación cenozoica en la región de Huimilpan, Querétaro y su relación con la sismicidad local: Revista Mexicana de Ciencias Geológicas, 22-2, 129-147.

Dawers, N.H., Anders, M.H., Scholz, C.H., 1993, Growth of normal faults: Displacement-length scaling: Geology, 21, 1107-1110.

Ferrari, L., Conticelli, S., Vaggelli, C., Petrone, C., Manetti, P., 2000, Late Miocene mafic volcanism and intra-arc tectonics during the early development of the Trans-Mexican Volcanic Belt: Tectonophysics, 318, 161-185.

Ferrill, D.A., Morris, A.P., 2001, Displacement gradient and deformation in normal fault systems: Journal of Structural Geology, 23, 619-638.

Groshong, R.H., 1999. 3-D structural geology, New York. Springer.

Gupta, A., Scholz, C.H., 2000, A model of normal fault interaction based on observations and theory: Journal of Structural Geology, 22, 865-879.

Hernández, J., Carrasco-Núñez, G., Aguirre-Díaz, G., 2009, Dinámica eruptiva de la "Pómez Ezequiel Montes" en la caldera Amazcala, centro de México: Revista Mexicana de Ciencias Geológicas, 26, 482-500.

Higgs, W.G., Williams, G.D., Powell, C.M., 1991, Evidence for flexural shear folding associated with extensional faults: Bulletin of the Geologic Society of America. 103, 710-717.

Huggins, P., Watterson, J., Walsh, J.J., Childs, C.J., 1995, Relay zone geometry and displacement transfer between normal faults recorded in coal-mine plans: Journal of Structural Geology, 17, 1741-1755.

Hus, V., Acocella, R., Funiciello, De Batist. M., 2005, Sandbox models of relay ramp structure and evolution: Journal of Structural Geology, 27, 459–473

Kristensen, M.B., Childs, C.J., Korstgard, J.A., 2008, The 3D geometry of small-scale relay zones between normal faults in soft sediments: Journal of Structural Geology, 30, 257-272

Johnson, C.A., Harrison, C.G.A., 1990, Neotectonics in central México: Physics of the Earth Interior, 64, 187–210.

Larsen, P.-H., 1988, Relay structures in a Lower Permian basement-involved extension system, East Greenland: Journal of Structural Geology, 10, 3-8.

Maerten, L., Willemse, E.J.M., Pollard, D.D., Rawnsley, K., 1999, Slip distributions on intersecting normal faults: Journal of Structural Geology, 21, 259-271.

Peacock, D.C.P., Parfitt, E.A., 2002, Active relay ramps and normal fault propagation on Kilauea Volcano, Hawaii: Journal of Structural Geology, 24, 729-742.

Peacock, D.C.P., Sanderson, D.J., 1991, Displacements, segment linkage and relay ramps in normal fault zones: Journal of Structural Geology, 13, 721-733.

Peacock, D.C.P., Sanderson, D.J., 1993, Estimating strain from fault slip using a line sample: Journal of Structural Geology, 12, 1513-1516.

Peacock, D.C.P., Sanderson, D.J., 1994, Geometry and development of relay ramps in normal fault systems: The American Association of Petroleum Geologist Bulletin, 78, 147–165.

Rykkelid, E., Fossen, H., 2002, Layer rotation around vertical fault overlap zones: observations from seismic data, field examples and physical experiment: Marine and Petroleum Geology, 19, 181-192.

Segall, P., Pollard, D.D., 1983, Joint formation in granitic rock of the Sierra Nevada: Geological Society of America Bulletin, 94, 563-575.

Soliva, R., Benedicto, A., 2005, Geometry, scaling relations and spacing of vertically restricted normal faults: Journal of Structural Geology, 27, 317-325.

Suter, M., Quintero, O., López, M., Aguirre-Díaz, G.J., Farrar, E., 1995, The Acambay graben: Active intra-arc extension in the trans-Mexican volcanic belt, Mexico: Tectonics, 14, 1245–1262.

Suter, M., López-Martínez, M., Quintero-Legorreta, O., Carrillo-Martínez, M., 2001, Quaternary intra-arc extension in the central Trans-Mexican Volcanic Belt: Geological Society of America Bulletin, 113, 693–703.

Walsh, J.J., Watterson, J., Bailey, W.R., Childs, C.J., 1999, Fault relays, bends and branch-lines: Journal of Structural Geology, 21, 1019-1026.

Westaway, R., Kusznir, N., 1993, Fault and bed "rotation" during continental extension: block rotation or vertical shear?: Journal of Structural Geology, 15, 753-770.

White, N.J., Jackson, J.A., Mckenzie, D.P., 1986, The relationship between the geometry of normal faults and that of the sedimentary layers in their hanging walls: Journal of Structural Geology, 8, 879-909.

Wojtal, S., 1989, Measuring displacement gradients and strains in faulted rocks: Journal Structural Geology, 11, 669--678.

Xu, S-S., Nieto-Samaniego, A.F., Alaniz-Álvarez, S.A., 2004. Vertical shear mechanism of faulting and estimation of strain in the Sierra de San Miguelito, Mesa Central, Mexico: Geological Acta, 2, 189-201.

Xu, S-S., Nieto-Samaniego, A.F., Alaniz-Álvarez, S.A., 2010, 3D Mohr diagram to explain reactivation of pre-existing planes due to changes in applied stresses, *in* Xie, F. (ed.) Rock Stress and Earthquakes: London. Taylor & Francis Group, 739-745.

Manuscrpt received: April 4, 2010
Corrected manuscript received: March 31, 2011
Manuscript accepted: April 5, 2011

Erratum / *Fe de erratas*

Erratum to Structural analysis of a relay ramp in the Querétaro graben, central Mexico: Implications for relay ramp development [Rev. Mex. Cienc. Geol., 28 (2011), 275-289][a]

Shunshan Xu*, Ángel Francisco Nieto-Samaniego, Susana Alicia Alaniz-Álvarez, and Luis Mariano Cerca-Martínez

Universidad Nacional Autónoma de México, Centro de Geociencias, Apartado Postal 1-742, Querétaro, Qro., 76001, México.
** sxu@geociencias.unam.mx*

In the above article, Table 1 was inadvertently omitted in the final version online and in print. This table appears below and also has been attached to the online version of the paper. The publisher and authors apologize for the oversight.

En el artículo indicado arriba no se incluyó la Tabla 1, tanto en la versión impresa como en la electrónica. Esta tabla se reproduce abajo y ha sido anexada a la versión electrónica del artículo. Los editores y los autores lamentan la omisión.

Table 1. Calculated extension of eight observed sections.

Section	**1**	**2**	**3**	**4**	**5**	**6**	**7**	**8**
Length *L* (m)	86.83	100.3	20	176.6	68.6	60	200	160
Number of veins and dykes	65	61	10	20	66	54	77	37
Total width *W* (m)	1.61	2.23	0.72	2.95	0.99	1.48	1.91	0.81
Extension *e*	0.019	0.023	0.037	0.017	0.015	0.025	0.010	0.005

[a] Artículo original: http://rmcg.unam.mx/28-2/(09)Xu.pdf

Xu, S-S., Nieto-Samaniego, A.F., Alaniz-Álvarez, S.A., Cerca-Martínez, L.M., 2013, Erratum to Structural analysis of a relay ramp in the Querétaro graben, central Mexico: implications for relay ramp development: Revista Mexicana de Ciencias Geológicas, v. 30, núm. 3, p.614.